Extensivity of Energy and Electronic and Vibrational Structure Methods for Crystals

So Hirata, Murat Keçeli, Yu-ya Ohnishi, Olaseni Sode, and Kiyoshi Yagi

Department of Chemistry, University of Illinois at Urbana-Champaign, Urbana, Illinois 61801; email: sohirata@illinois.edu

Annu. Rev. Phys. Chem. 2012. 63:131–53

First published online as a Review in Advance on January 3, 2012

The *Annual Review of Physical Chemistry* is online at physchem.annualreviews.org

This article's doi: 10.1146/annurev-physchem-032511-143718

0066-426X/12/0505-0131$20.00

Keywords

extensive quantities, intensive quantities, lattice sums, thermodynamic limit, size consistency, diagrams

Abstract

A pedagogical proof is presented for the extensivity of energies of metallic and nonmetallic crystals that proceeds by elucidating the asymptotic distance dependence of the effective chemical interactions: kinetic, Coulomb, exchange, and correlation. On this basis, a guideline for the size-consistent design of electronic and vibrational methods is proposed. This guideline underscores the significance of the distinct use of the intermediate and standard normalization of wave functions for extensive and intensive quantities, includes the extensive and intensive diagram theorems as the unambiguous criteria for determining size consistency of a method for extensive and intensive quantities, and introduces the extensive-intensive consistency theorem, which stipulates the precise balance between the determinant spaces reached by extensive and intensive operators. Electronic and vibrational methods for crystals are reviewed that are inspired by these formal analyses or developed in accordance with the guideline.

1. INTRODUCTION

HF: Hartree–Fock

SCF: self-consistent field

MP: Møller–Plesset perturbation

CI: configuration interaction

CC: coupled cluster

DFT: density-functional theory

VMP: vibrational Møller–Plesset perturbation

VCC: vibrational coupled cluster

Size consistency: a desirable property that a method is said to possess when it predicts thermodynamic observables having the correct volume dependence

The objective of electronic structure theory is to solve the time-independent Schrödinger equation of a chemical system in its electronic degrees of freedom, which can be separated from the rest by the Born–Oppenheimer approximation. This may be followed by solving the time-independent Schrödinger equation in the nuclear degrees of freedom, taking into account the effects of anharmonicity in a bound potential energy surface (PES). This is done by vibrational structure theory. Some representative approximations of electronic and vibrational structure theories include Hartree–Fock (HF) or self-consistent field (SCF) theory, Møller–Plesset perturbation (MP) theory, configuration-interaction (CI) theory, and coupled-cluster (CC) theory.

There is an inevitable trade-off between the accuracy of these approximations and their applicability to larger chemical systems. Generally, less accurate methods such as density-functional theory (DFT) for electrons and the harmonic approximation for vibrations are more widely applicable to large systems, which today include solids and even liquids. In contrast, systematically accurate and thus predictive approximations such as electronic and vibrational MP, CI, and CC methods have been limited to rather small molecules in the gas phase. The primary task of computational quantum chemists and computational solid-state physicists is to push this accuracy–applicability trade-off curve in the direction of greater accuracy and wider applicability. This requires innovation in theories and algorithms tailored to the chemistry and physics of the systems under consideration as well as more general computer science optimizations such as parallelism.

Today, the accuracy–applicability trade-off is reaching a point in which we face the exciting prospect of having polymers, solids, and perhaps even liquids in the applicable domain of electronic many-body methods that go beyond DFT and of vibrational many-body methods that go beyond the harmonic approximation and are based on accurate PES. These many-body methods differ from more empirical or semiempirical approximations, which have thus far been predominantly used for condensed matter. The distinguishing feature of the former methods is that their accuracy is subject to systematic improvements. For small molecules in the gas phase, this control of accuracy has been routinely demonstrated to the extent that the calculated results can be brought to essentially exact agreement with the observed (1).

Having witnessed the impact of these methods on molecular sciences, chemists should have little doubt that the corresponding methods for polymers and solids can transform the quantitative aspects of materials science. To be more specific, DFT, long a workhorse of solid state physics, is fundamentally limited in its ability to reproduce energy bands and band gaps, the very properties materials scientists care about the most. There is ample evidence that MP and CC methods can resolve this issue for insulators and semiconductors (2). In molecular crystals, the strength of chemical interactions that are important in determining their structures span three orders of magnitude. Perhaps only CC methods are known to be capable of reproducing all of these interactions simultaneously with sufficient accuracy (3, 4).

Anharmonicity in the PES of a solid is responsible for such important phenomena as thermal expansion, thermal conductivity, and specific heat at high temperatures. Besides supplying the quantitatively accurate anharmonic PES, the MP and CC methods suggest that their underlying mathematical descriptions of wave functions can be applied directly to those of anharmonic lattice vibrations, leading to vibrational Møller–Plesset perturbation (VMP) and vibrational coupled-cluster (VCC) methods (5, 6).

To fully realize these electronic and vibrational many-body methods for solids, one must pay close attention to the issue of size consistency (7–10) in addition to the obviously crucial question of how to contain the enormous computational costs of these methods when applied to very large systems. Size consistency is the single most important guideline for the design of electronic and

vibrational methods. It is the property a method is said to possess when it yields observable quantities that scale correctly with the size (volume) of the system. For instance, thermodynamically extensive quantities such as energy and entropy are asymptotically proportional to the volume of the system, whereas intensive quantities such as energy density, excitation energies, pressure, and temperature are asymptotically constant (11). Size-consistent methods are the ones that yield energies that are extensive, excitation energies that are intensive, and so on. Only these methods can maintain uniform accuracy across system size all the way to infinity and be safely applied to solids. Conversely, methods that are not size consistent yield calculated values of observables that have an increasing proportion of errors and reduce to a sheer nonsense in the thermodynamic (infinite-volume) limit.

Extensive quantity: a thermodynamic observable of a chemical system that is asymptotically directly proportional to the volume of the system

Intensive quantity: a thermodynamic observable of a chemical system that is asymptotically independent of the volume of the system

In Section 3 of this review, we summarize the guideline for the size-consistent design in the form of algebraic or diagrammatic theorems—some existing and others new—that should be generally applicable to methods that are meant to predict thermodynamic observables (10).

However, before doing so, we must address the more fundamental question as to why the energy of a chemical system is extensive and, therefore, the theory of thermodynamics can be applied to chemistry (12). To many readers, this question may seem easy to answer or too elementary to be relevant for practical computational methodologies. This is far from true! It took 40 years for the finest mathematicians (including a Fields medalist) to complete the proof of extensivity of energy or, equivalently, the existence of a constant thermodynamic (infinite-volume) limit of energy density (13–17). This is, therefore, an extremely tough question to answer.

We must recognize that to prove this for an arbitrary assembly of interacting particles is impossible for the simple reason that energy is not always extensive. Energy is extensive basically only for electrically neutral chemical systems, in which attractive and repulsive interactions cancel each other nearly exactly, leaving behind effective interactions that decay sufficiently rapidly to suppress divergence in the interaction (lattice) sums of energy density. The proof therefore requires an understanding of the asymptotic decay behavior of these effective interactions—an understanding that is not only relevant but also critical for constructing intelligent algorithms and approximations of electronic and vibrational structure methods for large systems. The cost of accurate calculations is, in fact, ultimately determined by the slowest decaying component, whose nature and asymptote seem to vary depending on whether the system is metallic.

This review therefore begins with an analysis in Section 2 of the asymptotic decay behavior of effective interactions, namely, the kinetic, Coulomb, and exchange interactions in the HF theory as well as the correlation interactions obtainable from the MP or CC method, in an electrically neutral, perfect crystal. We provide a proof that the sum of these interactions, which equals the exact total energy of the crystal, is extensive. It is based on some strong assumptions about the shape of the Fermi surface and the canonical HF spin-orbitals and, in this sense, is more restrictive than the aforementioned mathematical proofs. It is, however, more accessible and directly relevant for chemists and physicists who develop efficient and size-consistent approximations of electronic and vibrational structure methods.

In Section 4, we survey examples of the methods we have recently developed, which are either inspired by or consistent with the formal analysis of extensivity and the general design guidelines for size-consistent methods.

2. EXISTENCE OF THERMODYNAMIC LIMIT

Why is energy extensive (12, 17–23)? Let us examine this question by taking as an example the three-dimensional (3D) equidistant lattice of particles attracting or repelling one another through pairwise interactions. The total energy (E) of this lattice is the sum of all distinct pairwise

Lattice sum: an infinite sum of particle-particle interactions in a periodic crystal

Thermodynamic limit: the limit in which the volume of a chemical system tends to infinity while the number density and chemical composition are held fixed

interactions. Because the number of such interactions increases quadratically, not linearly, with the number of particles, we may naively expect the total energy to grow more (but not exactly) quadratically than linearly with the volume (V). In fact, it may be somewhat surprising that the energy is observed to be extensive, given the quadratic increase of the distinct particle-particle interactions.

Another way to ask the same question is to ask why energy density (E/V) is intensive. The energy density of the lattice of particles is the sum of all distinct pairwise interactions between an arbitrary chosen "central" particle and all the other particles in the lattice. If the interaction decays as $1/r^n$, where r is the particle-particle distance, the question becomes a mathematical one: does the 3D lattice sum of the form

$$\sum_{\mathbf{m}}^{V} \frac{1}{|\boldsymbol{r}_{\mathbf{m}}|^n} \tag{1}$$

converge at a finite and thus V-independent thermodynamic limit? Here, $\mathbf{m}$ is a composite of three integers (m_x, m_y, and m_z) specifying a unit cell in the lattice and $\boldsymbol{r}_{\mathbf{m}}$ is the $\mathbf{m}$-th unit-cell vector (each unit cell contains a particle and has a unit volume). It converges if the integral,

$$\int_{x_0}^{\infty} dx \int_{y_0}^{\infty} dy \int_{z_0}^{\infty} dz \frac{1}{r^n}, \tag{2}$$

does, where x_0, y_0, and z_0 are positive real numbers that mark the onset of the asymptotic regime. We can answer this easily by switching from Cartesian coordinates to spherical coordinates. In the latter, what we must test is the convergence of the integral,

$$\int_{r_0}^{\infty} 4\pi r^2 dr \frac{1}{r^n}, \tag{3}$$

where r_0 is the onset of the asymptotic regime and $4\pi r^2$ is the volume element. We can carry out this integration analytically using high school calculus, arriving at the following conclusion: The integral converges at a finite thermodynamic limit, and therefore the energy density is intensive, if and only if $n > 3$ (17, 21). Otherwise, the thermodynamic limit of energy density does not exist; the total energy is not extensive and grows faster than linearly.

Interaction Asymptote Theorem I (17, 21): The energy density of a lattice of particles is finite when the particle-particle interaction decays as $1/r^n$ asymptotically with $n > 3$.

Two of our most familiar interactions in nature, namely, Coulomb and gravitational interactions, exhibit the slow $1/r$ decay. In a 3D lattice of masses or that of electrons, energy density would diverge and energy would be nonextensive. Insofar as the whole theory of thermodynamics is based on the premise that energy is extensive, thermodynamics would not work for these systems (24). As mentioned above, energy is extensive essentially only for electrically neutral systems in which attractive interactions between oppositely charged particles and repulsive interactions between like-charged particles cancel to a great extent, with the remaining effective interactions decaying rapidly.

However, even in such systems, the energy can and will cease to be extensive once their volumes become so large that the gravitational interactions cannot be neglected. Thermodynamics, therefore, does not apply to very large systems. It does not apply to very small systems, either, because the cancellation between attractive and repulsive Coulomb interactions may not be complete. Such small systems include electrons in an isolated atom or molecule, which should be distinguished from an ensemble of atoms or molecules or electrons in a solid, for which thermodynamics

certainly works. It seems that thermodynamics has a certain limited domain of applicability in terms of system size and composition.

Nevertheless, if we confine ourselves to electrically neutral systems that are neither too small nor too large, we can indeed prove the extensivity of energy or the existence of thermodynamic limit of energy density. The problem was posed in mathematical terms by Fisher & Ruelle (17) in 1966 and by Dyson & Lenard (18) in 1967. The proof for mobile electrons and nuclei (overall electrically neutral) was obtained by Lebowitz & Lieb (13) in 1969. The proof for perfect crystals, namely, mobile electrons and a lattice of fixed nuclei, turned out to be harder but was proposed by Fefferman (14) in 1985. Only in 2009 was the proof made whole by Hainzl et al. (15, 16), who showed the existence of thermodynamic limit for perfect crystals and crystals with defects. We have also obtained a proof for perfect crystals (S. Hirata & Y.Y. Ohnishi, manuscript in preparation), which might be less rigorous in the sense that we have made a number of assumptions and simplifications but which is, in our view, more directly useful for our purpose of developing practical computational methodologies for solids because we have clarified the asymptotic decay of each of the effective interactions. Our proof is so simple that it can be reproduced in an abridged form in the following.

The task at hand is to show that the energy density (E/V) of a 3D crystal with electrically neutral unit cells remains finite and thus independent of V. We shall do this for individual energy components of the exact energy, namely, the kinetic, Coulomb, and exchange energies in the HF theory as well as the second- and all higher-order MP corrections (8) thereto:

$$E = E_{\mathrm{HF}} + \sum_{m=2}^{\infty} E_{\mathrm{MP}}^{(m)}, \tag{4}$$

$$E_{\mathrm{HF}} = E_{\mathrm{kinetic}} + E_{\mathrm{Coulomb}} + E_{\mathrm{exchange}}. \tag{5}$$

We use the atomic units throughout.

The kinetic energy of the crystal, E_{kinetic}, is the sum of the kinetic-energy integrals in the atomic spin-orbitals over all V unit cells. Hence,

$$E_{\mathrm{kinetic}} = -\frac{1}{2} \sum_{\mu,\nu} \sum_{\mathbf{m_1}}^{V} \sum_{\mathbf{m_2}}^{V} D_{\mu\mathbf{m_1}}^{\nu\mathbf{m_2}} \int d\boldsymbol{x} \chi_{\mu\mathbf{m_1}}^{*}(\boldsymbol{x}) \nabla^2 \chi_{\nu\mathbf{m_2}}(\boldsymbol{x}), \tag{6}$$

where each atomic spin-orbital, $\chi_{\mu\mathbf{m_1}}$, is chosen to be spatially strongly localized in unit cell $\mathbf{m_1}$, $\boldsymbol{x}$ represents the spin-orbital coordinates of an electron, and $D_{\mu\mathbf{m_1}}^{\nu\mathbf{m_2}}$ is the density matrix element to be defined and examined in detail later. Owing to the translational invariance of the basis, the kinetic energy per volume or the kinetic energy per unit cell is simply

$$\frac{E_{\mathrm{kinetic}}}{V} = -\frac{1}{2} \sum_{\mu,\nu} \sum_{\mathbf{m}}^{V} D_{\mu\mathbf{0}}^{\nu\mathbf{m}} \int d\boldsymbol{x} \chi_{\mu\mathbf{0}}^{*}(\boldsymbol{x}) \nabla^2 \chi_{\nu\mathbf{m}}(\boldsymbol{x}), \tag{7}$$

where a unit cell has a unit volume. This lattice sum is convergent at a finite, V-independent value because the kinetic-energy integral decays as rapidly with $\mathbf{m}$ as the does overlap between two spatially local atomic spin-orbitals. Therefore, the kinetic energy per volume is intensive and the kinetic energy is extensive.

We define the Coulomb energy as the sum of electron-electron repulsion, nucleus-nucleus repulsion, and electron-nucleus attraction energies. This is because, individually, these three components are always nonextensive for the crystal; only their sum may be extensive. Hence, we introduce the charge density of unit cell $\mathbf{0}$ that is the sum of the electron density and nuclear

charge density of the cell, namely,

$$\rho_{\mathbf{0}}(\boldsymbol{r}) = \rho_{\mathbf{0}}^{\mathrm{e}}(\boldsymbol{r}) + \rho_{\mathbf{0}}^{\mathrm{n}}(\boldsymbol{r}), \tag{8}$$

with

$$\rho_{\mathbf{0}}^{\mathrm{e}}(\boldsymbol{r}) = -\sum_{\mu,\nu}\sum_{\mathbf{m}}^{V} D_{\mu\mathbf{0}}^{\nu\mathbf{m}}\chi_{\mu\mathbf{0}}^{*}(\boldsymbol{x})\chi_{\nu\mathbf{m}}(\boldsymbol{x}), \tag{9}$$

$$\rho_{\mathbf{0}}^{\mathrm{n}}(\boldsymbol{r}) = \sum_{I=1}^{N} Z_I\delta(\boldsymbol{r} - \boldsymbol{r}_I + \boldsymbol{r}_{\mathbf{0}}), \tag{10}$$

where N is the number of nuclei in a unit cell; Z_I and $\boldsymbol{r}_I$ are, respectively, the charge and spatial coordinates of the I-th nucleus; and δ is the Dirac delta function. We assume that the electrical neutrality of unit cells,

$$\int d\boldsymbol{r}\rho_{\mathbf{0}}(\boldsymbol{r}) = 0. \tag{11}$$

This assumption is essential; without it, it is impossible to prove the extensivity of energy, because the energy of a crystal of a charged unit cell is nonextensive in the first place.

The Coulomb energy is written with this charge density as

$$E_{\mathrm{Coulomb}} = \frac{1}{2}\sum_{\mathbf{m_1}}^{V}\sum_{\mathbf{m_2}}^{V}\int\int d\boldsymbol{r}_1 d\boldsymbol{r}_2 \frac{\rho_{\mathbf{m_1}}(\boldsymbol{r}_1)\rho_{\mathbf{m_2}}(\boldsymbol{r}_2)}{|\boldsymbol{r}_1 - \boldsymbol{r}_2|} \tag{12}$$

or

$$\frac{E_{\mathrm{Coulomb}}}{V} = \frac{1}{2}\sum_{\mathbf{m}}^{V}\int\int d\boldsymbol{r}_1 d\boldsymbol{r}_2 \frac{\rho_{\mathbf{0}}(\boldsymbol{r}_1)\rho_{\mathbf{m}}(\boldsymbol{r}_2)}{|\boldsymbol{r}_1 - \boldsymbol{r}_2|}, \tag{13}$$

where it should be understood that the self-interactions of point charges are excluded. Because the charge density is net neutral, this last equation represents the sum of dipole-dipole interactions in the leading order of a multipole expansion (25). A dipole-dipole interaction has the asymptotic distance dependence of $1/r^3$. According to Asymptote Theorem I, this appears to cause a logarithmic divergence of the Coulomb energy density, but this is not the case. The theorem disregards any orientation dependence of the interactions. The orientation dependence of dipole-dipole interactions in a crystal is such that the angular integration of the interactions makes this contribution vanish identically (10). That is, the long-range part of this lattice sum is proportional to

$$\mu^2\int_{r_0}^{\infty} r^2 dr\int_0^{\pi}\sin\theta d\theta\int_0^{2\pi} d\phi\frac{1 - 3\cos^2\theta}{r^3} = 0, \tag{14}$$

where μ is the dipole moment of the unit cell. Therefore, the true leading-order contribution to the Coulomb energy density comes from quadrupole-quadrupole interactions with the $1/r^5$ asymptotic decay (25), whose lattice sum, according to Asymptote Theorem I, approaches a finite, intensive value. Hence, the Coulomb energy density is intensive and the Coulomb energy is extensive.

Interaction Asymptote Theorem II: The energy density of a lattice of particles is finite when the particle-particle interaction decays as $(1 - 3\cos^2\theta)/r^3$ asymptotically, where r and θ are the distance and inclination, respectively, in spherical coordinates.

The exchange energy is given by

$$E_{\text{exchange}} = -\frac{1}{2}\sum_{\mu,\nu,\kappa,\lambda}\sum_{\mathbf{m_1}}^{V}\sum_{\mathbf{m_2}}^{V}\sum_{\mathbf{m_3}}^{V}\sum_{\mathbf{m_4}}^{V} D_{\mu\mathbf{m_1}}^{\lambda\mathbf{m_4}} D_{\kappa\mathbf{m_3}}^{\nu\mathbf{m_2}} \int\int d\boldsymbol{x}_1 d\boldsymbol{x}_2 \frac{\chi^*_{\mu\mathbf{m_1}}(\boldsymbol{x}_1)\chi_{\nu\mathbf{m_2}}(\boldsymbol{x}_1)\chi^*_{\kappa\mathbf{m_3}}(\boldsymbol{x}_2)\chi_{\lambda\mathbf{m_4}}(\boldsymbol{x}_2)}{|\boldsymbol{x}_1 - \boldsymbol{x}_2|} \tag{15}$$

or

$$\frac{E_{\text{exchange}}}{V} = -\frac{1}{2}\sum_{\mu,\nu,\kappa,\lambda}\sum_{\mathbf{m_1}}^{V}\sum_{\mathbf{m_2}}^{V}\sum_{\mathbf{m_3}}^{V} D_{\mu\mathbf{0}}^{\lambda\mathbf{m_3}} D_{\kappa\mathbf{m_2}}^{\nu\mathbf{m_1}} \int\int d\boldsymbol{x}_1 d\boldsymbol{x}_2 \frac{\chi^*_{\mu\mathbf{0}}(\boldsymbol{x}_1)\chi_{\nu\mathbf{m_1}}(\boldsymbol{x}_1)\chi^*_{\kappa\mathbf{m_2}}(\boldsymbol{x}_2)\chi_{\lambda\mathbf{m_3}}(\boldsymbol{x}_2)}{|\boldsymbol{x}_1 - \boldsymbol{x}_2|}. \tag{16}$$

Remembering that the atomic spin-orbitals are spatially local, with their overlaps decaying rapidly, we see that the longest-range contributions to the lattice sum of Equation 16 include

$$-\frac{1}{2}\sum_{\mu,\kappa}\sum_{\mathbf{m}}^{V} |D_{\mu\mathbf{0}}^{\kappa\mathbf{m}}|^2 \int\int d\boldsymbol{x}_1 d\boldsymbol{x}_2 \frac{|\chi_{\mu\mathbf{0}}(\boldsymbol{x}_1)|^2 |\chi_{\kappa\mathbf{m}}(\boldsymbol{x}_2)|^2}{|\boldsymbol{x}_1 - \boldsymbol{x}_2|}. \tag{17}$$

The decay of this contribution with $\mathbf{m}$ is determined to a great extent by the asymptotic distance dependence of the density matrix element, $D_{\mu\mathbf{0}}^{\kappa\mathbf{m}}$. To understand the convergence of exchange lattice sums, therefore, we must first clarify the distance dependence of the density matrix elements in nonmetallic (26–28) and metallic crystals (29).

A canonical HF spin-orbital, $\varphi_{i\boldsymbol{k}}$, is a completely delocalized function over the whole volume of the crystal with the well-defined momentum or wave vector, $\boldsymbol{k}$. It can be expanded by atomic spin-orbitals as

$$\varphi_{p\boldsymbol{k}}(\boldsymbol{x}) = \frac{1}{\sqrt{V}}\sum_{\mu}\sum_{\mathbf{m}}^{V} \exp(i\boldsymbol{k}\cdot\boldsymbol{r}_{\mathbf{m}}) C_{p\boldsymbol{k}}^{\mu}\chi_{\mu\mathbf{m}}(\boldsymbol{x}). \tag{18}$$

The density matrix in the same basis is given by

$$D_{\mu\mathbf{m_1}}^{\nu\mathbf{m_2}} = \frac{1}{V}\sum_{p}\sum_{\boldsymbol{k}}^{V} n_{p\boldsymbol{k}} C_{p\boldsymbol{k}}^{\mu^*} C_{p\boldsymbol{k}}^{\nu} \exp\{i\boldsymbol{k}\cdot(\boldsymbol{r}_{\mathbf{m_2}} - \boldsymbol{r}_{\mathbf{m_1}})\} \tag{19}$$

$$= \frac{1}{(2\pi)^3}\sum_{p}\int d\boldsymbol{k}\, n_{p\boldsymbol{k}} C_{p\boldsymbol{k}}^{\mu^*} C_{p\boldsymbol{k}}^{\nu} \exp\{i\boldsymbol{k}\cdot(\boldsymbol{r}_{\mathbf{m_2}} - \boldsymbol{r}_{\mathbf{m_1}})\}, \tag{20}$$

where $n_{p\boldsymbol{k}}$ is the electron occupancy (either 0 or 1) of the state $p\boldsymbol{k}$ and the domain of integration is the unit cell in the reciprocal space.

In a nonmetallic crystal, every band is either completely filled by electrons ($n_{p\boldsymbol{k}} = 1$) or completely vacant ($n_{p\boldsymbol{k}} = 0$). For an occupied band, therefore, Equation 20 becomes a Fourier transform. Assuming that $C_{p\boldsymbol{k}}^{\mu}$ does not vary with $\boldsymbol{k}$, we find

$$D_{\mu\mathbf{m_1}}^{\nu\mathbf{m_2}} = \sum_{p} n_{p\boldsymbol{k}} C_{p\boldsymbol{k}}^{\mu^*} C_{p\boldsymbol{k}}^{\nu} \delta(\boldsymbol{r}_{\mathbf{m_2}} - \boldsymbol{r}_{\mathbf{m_1}}), \tag{21}$$

where δ is again the Dirac delta function. The density matrix elements in a nonmetallic crystal therefore decay extremely rapidly with $|\boldsymbol{r}_{\mathbf{m_2}} - \boldsymbol{r}_{\mathbf{m_1}}|$.

In a metallic crystal, at least one band (say, the q-th band) is only partially occupied by electrons. For this band, Equation 20 is no longer a Fourier transform but is a "striped" Fourier transform. We can nevertheless carry out the integration of this equation analytically, assuming again that $C_{p\boldsymbol{k}}^{\mu}$ is invariant with $\boldsymbol{k}$ and furthermore that the Fermi surface is spherical. It is found (29, 30) that, under these assumptions, the density matrix is given by

$$D_{\mu\mathbf{m_1}}^{\nu\mathbf{m_2}} = \frac{k_f^3}{2\pi^2} C_{q\boldsymbol{k}}^{\mu^*} C_{q\boldsymbol{k}}^{\nu} \frac{j_1(k_f|\boldsymbol{r}_{\mathbf{m_2}} - \boldsymbol{r}_{\mathbf{m_1}}|)}{k_f|\boldsymbol{r}_{\mathbf{m_2}} - \boldsymbol{r}_{\mathbf{m_1}}|} + \sum_{p\neq q} n_{p\boldsymbol{k}} C_{p\boldsymbol{k}}^{\mu^*} C_{p\boldsymbol{k}}^{\nu} \delta(\boldsymbol{r}_{\mathbf{m_2}} - \boldsymbol{r}_{\mathbf{m_1}}), \tag{22}$$

where j_1 is the first-order spherical Bessel function,

$$j_1(x) = \frac{\sin(x)}{x^2} - \frac{\cos(x)}{x}. \tag{23}$$

This indicates that the density matrix elements in a metallic crystal decay in an oscillatory manner with the envelope being asymptotically proportional to $|\boldsymbol{r}_{\mathbf{m}_2} - \boldsymbol{r}_{\mathbf{m}_1}|^{-2}$.

Coming back to Equation 17, we observe that the lattice sum for the exchange energy density has two appearances of the density matrix element involving atomic spin-orbitals in unit cells **0** and **m**. These elements decay as $1/r^2$ in metals and much more rapidly in nonmetals (29). Taking into account the Coulomb decay, $1/|\boldsymbol{x}_1 - \boldsymbol{x}_2|$, we surmise that the summand of Equation 17 must decay as $1/r^5$ asymptotically or more rapidly with $r = |\boldsymbol{r}_{\mathbf{m}} - \boldsymbol{r}_{\mathbf{0}}|$. According to Asymptote Theorem I, we can therefore conclude that the exchange energy density is intensive and that the exchange energy is extensive in both metals and nonmetals.

So far, we have shown that the kinetic, Coulomb, and exchange energies are individually extensive, meaning that the HF energy as their sum (Equation 5) is also extensive. Furthermore, using the foregoing analysis, we can show that the Fock (f) integrals in the canonical HF spin-orbital basis are intensive (asymptotically proportional to V) and that the two-electron integrals (v) in the same basis are inversely extensive (asymptotically inversely proportional to V) insofar as they are defined by

$$f_{q\boldsymbol{k}_q}^{p\boldsymbol{k}_p} = -\frac{1}{2}\int d\boldsymbol{x}\varphi_{p\boldsymbol{k}_p}^*(\boldsymbol{x})\nabla^2\varphi_{q\boldsymbol{k}_q}(\boldsymbol{x}) + \sum_r \sum_{\boldsymbol{k}_r}^{V} n_{r\boldsymbol{k}_r} v_{q\boldsymbol{k}_q r\boldsymbol{k}_r}^{p\boldsymbol{k}_p r\boldsymbol{k}_r}, \tag{24}$$

$$v_{r\boldsymbol{k}_r s\boldsymbol{k}_s}^{p\boldsymbol{k}_p q\boldsymbol{k}_q} = \int\int d\boldsymbol{x}_1 d\boldsymbol{x}_2 \frac{\xi_{r\boldsymbol{k}_r}^{p\boldsymbol{k}_p}(\boldsymbol{x}_1)\xi_{s\boldsymbol{k}_s}^{q\boldsymbol{k}_q}(\boldsymbol{x}_2)}{|\boldsymbol{x}_1 - \boldsymbol{x}_2|} - \int\int d\boldsymbol{x}_1 d\boldsymbol{x}_2 \frac{\zeta_{s\boldsymbol{k}_s}^{p\boldsymbol{k}_p}(\boldsymbol{x}_1)\zeta_{r\boldsymbol{k}_r}^{q\boldsymbol{k}_q}(\boldsymbol{x}_2)}{|\boldsymbol{x}_1 - \boldsymbol{x}_2|}, \tag{25}$$

where we introduce the HF spin-orbital product, $\zeta_{q\boldsymbol{k}_q}^{p\boldsymbol{k}_p}$, and also its electrically neutral counterpart, $\xi_{q\boldsymbol{k}_q}^{p\boldsymbol{k}_p}$, given by

$$\zeta_{q\boldsymbol{k}_q}^{p\boldsymbol{k}_p}(\boldsymbol{x}) = \varphi_{p\boldsymbol{k}_p}^*(\boldsymbol{x})\varphi_{q\boldsymbol{k}_q}(\boldsymbol{x}), \tag{26}$$

$$\xi_{q\boldsymbol{k}_q}^{p\boldsymbol{k}_p}(x) = \zeta_{q\boldsymbol{k}_q}^{p\boldsymbol{k}_p}(\boldsymbol{x}) - \frac{\delta_{pq}\delta_{\boldsymbol{k}_p\boldsymbol{k}_q}}{nV}\sum_{\mathbf{m}}^{V}\rho_{\mathbf{m}}^{\mathrm{n}}(\boldsymbol{r}), \tag{27}$$

where n is the number of electrons in a unit cell. These definitions (10, 31, 32) differ from the standard definitions in many textbooks or implementations because in Equation 27, we subtract the nuclear charge density from electron density, which is necessary to ensure the consistent V^0 and V^{-1} dependence of f and v across all elements. Note also that these integrals in the canonical HF spin-orbital basis vanish unless momentum conservation conditions are satisfied by the wave vectors involved.

The HF energy can be written with these integrals as

$$\begin{aligned} E_{\mathrm{HF}} &= \sum_p \sum_{\boldsymbol{k}_p}^{V} n_{p\boldsymbol{k}_p} f_{p\boldsymbol{k}_p}^{p\boldsymbol{k}_p} - \frac{1}{2}\sum_{p,q}\sum_{\boldsymbol{k}_p}^{V}\sum_{\boldsymbol{k}_q}^{V} n_{p\boldsymbol{k}_p} n_{q\boldsymbol{k}_q} v_{p\boldsymbol{k}_p q\boldsymbol{k}_q}^{p\boldsymbol{k}_p q\boldsymbol{k}_q} \\ &= \frac{V}{(2\pi)^3}\sum_p \int d\boldsymbol{k}_p n_{p\boldsymbol{k}_p} f_{p\boldsymbol{k}_p}^{p\boldsymbol{k}_p} - \frac{V^2}{2(2\pi)^6}\sum_{p,q}\int\int d\boldsymbol{k}_p d\boldsymbol{k}_q n_{p\boldsymbol{k}_p} n_{q\boldsymbol{k}_q} v_{p\boldsymbol{k}_p q\boldsymbol{k}_q}^{p\boldsymbol{k}_p q\boldsymbol{k}_q}, \end{aligned} \tag{28}$$

which contain the nucleus-nucleus repulsion energy. We can easily verify (10) the extensivity of each term in the right-hand side: The first term has a single $\boldsymbol{k}$-integration of the V^0 quantity (f), which scales as V^1 overall and is extensive, and the second term involves a double $\boldsymbol{k}$-integration of the V^{-1} quantity (v), which also scales as V^1.

At this point, it may be useful to reflect on the four different expressions of the exact electronic Hamiltonian, namely, the first-quantized, second-quantized, normal-ordered, and diagrammatic forms in the order of the increasing degree of sophistication (33).

Evolution of the Hamiltonian. The first-quantized form is

$$\hat{H} = -\frac{1}{2}\sum_i \nabla_i^2 - \sum_i \sum_I \frac{Z_I}{|\boldsymbol{r}_i - \boldsymbol{r}_I|} + \sum_{i<j} \frac{1}{|\boldsymbol{r}_i - \boldsymbol{r}_j|} + \sum_{I<J} \frac{Z_I Z_J}{|\boldsymbol{r}_I - \boldsymbol{r}_J|}. \tag{29}$$

The second-quantized form is

$$\hat{H} = \sum_{I<J} \frac{Z_I Z_J}{|\boldsymbol{r}_I - \boldsymbol{r}_J|} + \sum_{p,q} b_q^p \hat{a}_p^\dagger \hat{a}_q + \frac{1}{4}\sum_{p,q,r,s} w_{rs}^{pq} \hat{a}_p^\dagger \hat{a}_q^\dagger \hat{a}_s \hat{a}_r. \tag{30}$$

The normal-ordered form is

$$\hat{H} = E_{\mathrm{HF}} + \sum_{p,q} f_q^p \{\hat{a}_p^\dagger \hat{a}_q\} + \frac{1}{4}\sum_{p,q,r,s} v_{rs}^{pq} \{\hat{a}_p^\dagger \hat{a}_q^\dagger \hat{a}_s \hat{a}_r\}. \tag{31}$$

The diagrammatic form is

$$\hat{H} = E_{\mathrm{HF}} + \quad + \quad . \tag{32}$$

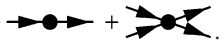

Note that the one- (b) and two-electron (w) integrals in Equation 30, whose definitions can be found elsewhere (7), differ from those in Equations 31 and 32 that are based on Equations 24 and 25. The most sophisticated forms—the normal-ordered and diagrammatic forms—are said to imply the fundamental significance of the HF energy expression, Equation 28, and the Fock integrals in electronic structure theory because they naturally emerge in these Hamiltonian expressions that are derived to expedite the evaluation of expectation values (33). The foregoing analysis suggests something more. The last two Hamiltonian expressions group terms according to their volume dependence: The first terms in Equations 31 and 32 are extensive (V^1 quantities), the second terms intensive (V^0), and the third terms inversely extensive (V^{-1}). The diagrammatic and underlying normal-ordered expressions are therefore superior to the other forms not only in the expediency they offer in formula derivations but also in the physics of size dependence that they embody.

With this preparation, let us complete the proof by showing the extensivity of the remaining energy component: correlation. The expression for the second-order MP (MP2) correlation correction to the HF energy for a crystal can be readily obtained by replacing each spin-orbital index in the molecular formula with the composite of a band index and a wave vector index and by inserting summations over distinct wave vectors (34–42). It reads

$$E_{\mathrm{MP}}^{(2)} = \frac{1}{4}\sum_{p,q,r,s} \sum_{\boldsymbol{k}_p}^{V} \sum_{\boldsymbol{k}_q}^{V} \sum_{\boldsymbol{k}_r}^{V} n_{p\boldsymbol{k}_p} n_{q\boldsymbol{k}_q} \bar{n}_{r\boldsymbol{k}_r} \bar{n}_{s\boldsymbol{k}_s} \frac{v_{p\boldsymbol{k}_p q\boldsymbol{k}_q}^{r\boldsymbol{k}_r s\boldsymbol{k}_s} v_{r\boldsymbol{k}_r s\boldsymbol{k}_s}^{p\boldsymbol{k}_p q\boldsymbol{k}_q}}{f_{p\boldsymbol{k}_p}^{p\boldsymbol{k}_p} + f_{q\boldsymbol{k}_q}^{q\boldsymbol{k}_q} - f_{r\boldsymbol{k}_r}^{r\boldsymbol{k}_r} - f_{s\boldsymbol{k}_s}^{s\boldsymbol{k}_s}}, \tag{33}$$

where $\bar{n}_{r\boldsymbol{k}_r} = 1 - n_{r\boldsymbol{k}_r}$. The fourth wave vector, $\boldsymbol{k}_s$, does not appear as a summation index as it is pinned down by the other three with the momentum conservation condition,

$$\boldsymbol{k}_p + \boldsymbol{k}_q - \boldsymbol{k}_r - \boldsymbol{k}_s = \boldsymbol{k}, \tag{34}$$

where $\boldsymbol{k}$ is a vector of translation in the reciprocal lattice of the crystal. The extensivity of $E_{\mathrm{MP}}^{(2)}$ (43) is now plain to see. Each of the two-electron integrals in the denominator contributes a factor of V^{-1} to the volume dependence of the expression, whereas the Fock integrals are V^0 quantities and do not alter it. The threefold $\boldsymbol{k}$-summation contributes a factor of V^3 to the volume dependence. Overall, Equation 33 scales as V^1 and is extensive. Equation 33 also explains the $1/r^6$ asymptotic

decay of the correlation interaction (cf. dispersion) (2, 38), given the $1/r^3$ falloff of the two-electron integrals in the atomic spin-orbital basis.

RPA: random-phase approximation

This logic can be readily extended to third- and higher-order corrections, $E_{\mathrm{MP}}^{(n)}$ ($n > 2$), thanks to Goldstone's linked diagram theorem (44). According to this theorem, the n-th-order perturbation correction to the energy is represented by a linked diagram with n two-electron integral vertexes and $n - 1$ denominators composed of the Fock integrals. It is not immediately obvious how many wave vectors are distinct and become independent summation indexes in these diagrams, but an inspection shows that there are $n + 1$ of them in a linked n-vertex diagram (10). Therefore, the volume dependence of $E_{\mathrm{MP}}^{(n)}$ is V^{-n} (from the n two-electron integrals) times V^0 (from $n - 1$ denominators) times V^{n+1} (from the summation over $n + 1$ wave vectors) or V^1 overall. We thus conclude that the correlation energy is also extensive. This completes our "chemical" proof of the extensivity of energy of a perfect crystal.

Finally, we must issue a caveat. MP2 and all higher-order corrections are known to diverge in a metal because of the singularities in expressions like Equation 33 on the Fermi surface (41, 42, 45). There are at least two known solutions to circumvent this divergence. One is to invoke Gell-Mann–Brueckner theorem (45), which states that the sum of all perturbation corrections, which are individually divergent, is finite for the homogeneous electron gas; this is only a formal solution. The other is to employ CC that sums divergent diagrammatic contributions even at its lowest-order approximation and is finite at any order for the homogeneous electron gas (45–47). Random-phase approximation (RPA) (48–52), which may be viewed as an approximation to CC doubles (CCD) (53, 54), does the same and is well behaved for metals.

3. SIZE-CONSISTENT DESIGN AND THEOREMS

What are the implications of the formal analysis in the above section on practical computational methods? In this section, we summarize them, some in the form of theorems, as they pertain to the size-consistent design of electronic and vibrational methods. For the derivation and more in-depth discussions of these, the readers are referred to Reference 10.

3.1. Charge-Consistent Fock and Two-Electron Integrals

Equations 24 and 25 exploit the electrical neutrality of unit cells at the integral level; this is necessary for each integral to have formally consistent, well-defined volume dependence. How will these new, charge-consistent definitions (10, 31, 32) of integrals affect electronic structure methods in practice?

The HF energy given by Equation 28, molecular orbitals, orbital energy differences, and correlation energies are unchanged by these new definitions. Only the diagonal Fock integrals or the orbital energies, $f_{p\boldsymbol{k}_p}^{p\boldsymbol{k}_p}$, are affected and differ from the ones in the conventional definition, $\tilde{f}_{p\boldsymbol{k}_p}^{p\boldsymbol{k}_p}$, but merely by a constant (32),

$$f_{p\boldsymbol{k}_p}^{p\boldsymbol{k}_p} = \tilde{f}_{p\boldsymbol{k}_p}^{p\boldsymbol{k}_p} + \frac{1}{n}\left(E_{\mathrm{en}} + 2E_{\mathrm{nn}}\right), \tag{35}$$

where E_{en} and E_{nn} are the electron-nucleus attraction and nucleus-nucleus repulsion energies, respectively, per unit cell, given by

$$E_{\mathrm{en}} = \sum_{\mathbf{m}}^{V} \int\int d\boldsymbol{r}_1 d\boldsymbol{r}_2 \frac{\rho_{\mathbf{0}}^{\mathrm{e}}(\boldsymbol{r}_1)\rho_{\mathbf{m}}^{\mathrm{n}}(\boldsymbol{r}_2)}{|\boldsymbol{r}_1 - \boldsymbol{r}_2|}, \tag{36}$$

$$E_{\mathrm{nn}} = \frac{1}{2}\sum_{\mathbf{m}}^{V} \int\int d\boldsymbol{r}_1 d\boldsymbol{r}_2 \frac{\rho_{\mathbf{0}}^{\mathrm{n}}(\boldsymbol{r}_1)\rho_{\mathbf{m}}^{\mathrm{n}}(\boldsymbol{r}_2)}{|\boldsymbol{r}_1 - \boldsymbol{r}_2|}, \tag{37}$$

from which the self-interactions of point charges are understood to be excluded. The Fock integrals in the new definition are shown to converge considerably more rapidly with respect to the number of unit cells included in the lattice sums (32). This is because the diagonal Fock integrals in the conventional definition contain the lattice sums of charge-quadrupole, charge-sextupole, etc., interactions, whereas those in the charge-consistent definition do not.

In addition to these formal and practical advantages, the definition explicitly prohibits physically unacceptable approximations in molecular integrals evaluation. In a number of electronic-structure programs for molecules, electron-repulsion integrals are often thrown out or never computed, either on the basis of their (predicted) small absolute values or at some cutoff distances between basis functions, without the corresponding removal of long-range electron-nucleus and nucleus-nucleus interactions, potentially introducing a catastrophic error in the energy density of a solid. The charge-consistent definitions of Equations 24 and 25 make it more difficult to suggest such approximations. One demerit of the definitions is that Koopmans' theorem no longer applies.

3.2. Normalization of Wave Functions

There are two schemes of normalization of wave functions—the intermediate and standard normalizations—that are in use in electron-correlation theories (7). A wave function, Ψ, that is subject to intermediate normalization is not normalized; only its reference Slater determinant, Φ, is normalized:

$$\Psi = \Phi + \sum_{i=1}^{n} \sum_{a=n+1}^{\infty} t_i^a \Phi_i^a + \frac{1}{4} \sum_{i,j=1}^{n} \sum_{a,b=n+1}^{\infty} t_{ij}^{ab} \Phi_{ij}^{ab} + \cdots \tag{38}$$

and

$$\langle \Psi | \Phi \rangle = 1, \tag{39}$$

where Φ_i^a and Φ_{ij}^{ab} are singly and doubly excited Slater determinants with associated excitation amplitudes, t_i^a and t_{ij}^{ab}, respectively. This intermediate normalization seems almost mandatory in MP and CC methods for the ground states.

A wave function in the standard normalization can be written as

$$\Psi = \sum_{i=1}^{n} \sum_{a=n+1}^{\infty} c_i^a \Phi_i^a + \frac{1}{4} \sum_{i,j=1}^{n} \sum_{a,b=n+1}^{\infty} c_{ij}^{ab} \Phi_{ij}^{ab} + \cdots \tag{40}$$

and

$$\langle \Psi | \Psi \rangle = 1. \tag{41}$$

This is employed (sometimes implicitly) in the CI methods for the ground and excited states.

Why do we have these two schemes, and what are the essential differences between the two? Here are the answers (10): The excitation amplitudes (t) in the wave function intermediately normalized and those (c) in the wave function normalized have different volume dependence. The difference is such that we must use the intermediate normalization when describing extensive quantities such as correlation energies in the ground state, whereas we should use the standard normalization for intensive quantities such as excitation energies. We thus advocate calling excitation operators, amplitudes, and vertexes that appear in an intermediately normalized wave function extensive operators, extensive amplitudes, and extensive vertexes. The corresponding quantities in a normalized wave function are intensive operators, intensive amplitudes, and intensive vertexes. An n-th-order extensive vertex is shown to have the volume dependence of $V^{1-n/2}$, whereas an n-th-order intensive vertex is a $V^{1/2-n/2}$ quantity (10).

Normalization Theorem (10): The amplitudes of an extensive operator are subject to intermediate normalization and scale as $V^{1-n/2}$ where n is the number of external edges of the corresponding vertex. The amplitudes of an intensive operator are normalized and scale as $V^{1/2-n/2}$. The Hamiltonian is an extensive operator.

Connected diagram: a diagram in which a path exists between any pair of vertexes

3.3. Extensive and Intensive Diagram Theorems

The volume dependence of the vertexes of extensive and intensive operators leads us to the convenient, foolproof diagrammatic criteria by which to judge whether a given method is size consistent.

Extensive Diagram Theorem (33, 44): The equations defining a size-consistent method for extensive quantities consist only of connected diagrams with no intensive vertexes.

This is well known and a part of Goldstone's linked diagram theorem. As an example of electronic-structure methods that satisfy this theorem, let us consider linearized CCD (LCCD). Its energy and amplitude equation are diagrammatically given by

$E_{\mathrm{LCCD}} = E_{\mathrm{HF}} +$  , (42)

and

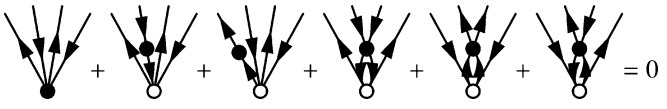 . (43)

Here, the filled and open circles are the Hamiltonian and two-electron excitation vertexes, respectively, which are both extensive vertexes. Each diagram is connected, proving immediately that LCCD is size consistent for extensive correlation energies.

We have introduced the corresponding theorem for intensive quantities.

Intensive Diagram Theorem (10): The equations defining an intensive quantity of a size-consistent method consist of connected diagrams with two intensive vertexes. The equations that determine the intensive amplitudes may be disconnected but must consist of one connected open part with one intensive vertex and any number of connected closed parts, each with two intensive vertexes.

CI singles (CIS) is an example of size-consistent methods for intensive quantities (excitation energies, in this case). It can be diagrammatically defined by

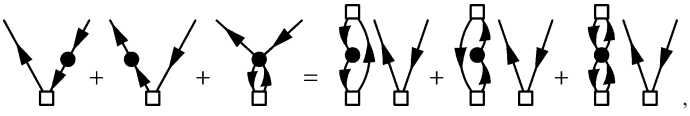 , (44)

where the open squares are the one-electron excitation vertexes, which are intensive vertexes subject to standard normalization. The diagrams on the right-hand side are disconnected (as well as unlinked), yet they satisfy the intensive diagram theorem. So do the diagrams on the left-hand side. This proves the size consistency of CIS for intensive excitation energies.

3.4. Consistency of Extensive and Intensive Operators

Often, we are interested in describing excitation, dissociation, and other intensive properties, while capturing correlation effects in the reference (ground) states, which are extensive. How can we define a method that is simultaneously size consistent for extensive and intensive quantities and hence satisfies the extensive and intensive diagram theorems?

A wave function of such a method must involve both extensive and intensive amplitudes that are subject to intermediate and standard normalization, respectively. It may be written as

$$\Psi = \hat{C}(1 + \hat{T})\Phi, \tag{45}$$

where $\hat{T}$ is the extensive operator, whose amplitudes are determined first by extensive methods such as MP and CC, before the amplitudes of the intensive operator, $\hat{C}$, are obtained by a CI procedure. For this method to be size consistent for both extensive and intensive quantities simultaneously, the spaces of the Slater determinants reachable by $\hat{T}$ and $\hat{C}$ must conform to the following theorem.

Extensive-Intensive Consistency Theorem (10): The CI equations that determine the amplitudes of the intensive operator, $\hat{C}$, must have the trivial solution, $\hat{C} = 1$, within the space of Slater determinants that can be reached by $\hat{C}^{\dagger}\hat{C}$ from Φ.

This condition may be violated if the space reached by $\hat{C}$ is too large as compared with that accessible by $\hat{T}$. In this case, $\hat{C}$ attempts to improve the description of correlation in the ground state, which is extensive, in addition to expressing intensive processes. The intensive operator, $\hat{C}$, is not equipped to achieve this in a size-consistent fashion. In other words, for a method to be size consistent, $\hat{C}$ must not be allowed to improve the energy of the reference (ground) state.

There is a class of methods that are designed in completely different philosophies. A number of the so-called multireference methods perform a truncated CI or related nonextensive procedure first for the reference (ground) state, before correlation corrections are made by MP or CC. The energy of the reference state tends to be plagued by nonextensive contributions from the outset. The above theorem tends not to be satisfied by such methods.

4. EXAMPLES OF SIZE-CONSISTENT METHODS

4.1. Size-Consistent Anharmonic Vibrational Methods

In the molecular electronic structure community, the significance of size consistency and the power of diagrammatic many-body methods have been well recognized thanks to the effort of pioneers such as Bartlett, who wrote one of the most highly cited reviews in this series on the subject (8). We have MP and CC methods and various combinations for electron correlation in the ground states and CC methods and CIS for excited states, many of which have been implemented for and applied to crystals under the periodic boundary conditions: MP2 (34–42), third-order MP (MP3) (39, 55, 56), fourth-order MP (MP4) (55), CC singles and doubles (CCSD) (39), explicitly correlated MP2 (57), CIS (58–61), and CCSD for excited states (62). For molecular anharmonic vibrational methods, however, the issues of size consistency are only beginning to be addressed (6).

The vibrational counterpart of the SCF theory is called vibrational self-consistent field (VSCF) (63–65). It approximates a vibrational wave function by a normalized product of 1D functions of

normal coordinates, φ, or modals:

VSCF: vibrational self-consistent field

$$\Psi(Q_1, \ldots, Q_n) = \prod_{i=1}^{n} \varphi_i(Q_i), \tag{46}$$

where n is the number of modes and Q_i is the i-th normal coordinate. The shape of each modal is varied so as to minimize the expectation value of the vibrational Hamiltonian in the VSCF wave function. This amounts to solving the one-mode VSCF equation for each modal,

$$\left\{-\frac{1}{2}\frac{\partial^2}{\partial Q_i^2} + V_i(Q_i)\right\} \varphi_i(Q_i) = E_i \varphi_i(Q_i), \tag{47}$$

which couples with one another through the effective one-mode potential, V_i, given by

$$V_i(Q_i) = \langle \Psi_i | V(Q_1, \ldots, Q_n) | \Psi_i \rangle \tag{48}$$

with

$$\Psi_i(Q_1, \ldots, Q_{i-1}, Q_{i+1}, \ldots, Q_n) = \frac{\Psi(Q_1, \ldots, Q_n)}{\varphi_i(Q_i)}, \tag{49}$$

where V is the PES. The total energy is the expectation value,

$$E = \langle \Psi | \hat{H} | \Psi \rangle. \tag{50}$$

VSCF can account for the effects of weak anharmonicity in the PES on the vibrational energies in the ground state (the sum of zero-point energies) and vibrational transition energies as well as vibrationally averaged molecular properties. It also serves as the reference wave function for subsequent vibrational "correlation" methods such as VMP (66, 67) and VCC (68).

Is VSCF size consistent? To answer this, we must know the volume dependence of the PES, which seems possible only when we expand it in a Taylor series:

$$\begin{aligned} \hat{H} = E_0 &+ \sum_{i=1}^{n} F_i Q_i + \frac{1}{2!}\sum_{i,j=1}^{n}\left\{-\delta_{ij}\frac{\partial^2}{\partial Q_i^2} + F_{ij} Q_i Q_j\right\} + \frac{1}{3!}\sum_{i,j,k=1}^{n} F_{ijk} Q_i Q_j Q_k \\ &+ \frac{1}{4!}\sum_{i,j,k,l=1}^{n} F_{ijkl} Q_i Q_j Q_k Q_l + \cdots, \end{aligned} \tag{51}$$

where E_0 is the electronic energy at the equilibrium geometry and F_i, F_{ij}, F_{ijk}, and F_{ijkl} are force constants. Diagrammatically, this is expressed as

$\hat{H} = E_0 +$ 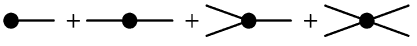 $+ \cdots.$ (52)

As stated above, the Hamiltonian is an extensive operator and its n-th-order vertex displays $V^{1-n/2}$ volume dependence. At this point, it may be clear that the total energy of VSCF, Equation 50, cannot be rigorously extensive because, for instance, the second and fourth terms of Equations 51 or 52, which involve odd-order force constants, cannot form closed, connected diagrams. This may become more evident in the next equation in which we show how closed diagrams can indeed be formed from the right force constants. In Reference 6, we show algebraically that the VSCF energy and one-mode equation have numerous terms that have nonphysical size dependence.

We thus introduce extensive VSCF (XVSCF) (69), which is diagrammatically size consistent for both total (zero-point) and transition energies. Its total energy is diagrammatically

$$E = E_0 +$$ 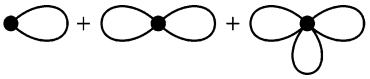 $$+ \cdots ,$$ (53)

and algebraically

$$E = E_0 + \frac{1}{2}\sum_{i=1}^{n}\left(-\left\langle\varphi_i\left|\frac{\partial^2}{\partial Q_i^2}\right|\varphi_i\right\rangle + \langle\varphi_i\,|\,Q_i^2\,|\,\varphi_i\rangle\right) + \frac{1}{2!2^2}\sum_{i,j=1}^{n} F_{iijj}\langle\varphi_i\,|\,Q_i^2\,|\,\varphi_i\rangle\langle\varphi_j\,|\,Q_j^2\,|\,\varphi_j\rangle$$
$$+\frac{1}{3!2^3}\sum_{i,j,k=1}^{n} F_{iijjkk}\langle\varphi_i|Q_i^2|\varphi_i\rangle\langle\varphi_j|Q_j^2|\varphi_j\rangle\langle\varphi_k|Q_k^2|\varphi_k\rangle + \cdots, \quad (54)$$

which contains only even-ordered force constants of certain types and satisfies the extensive diagram theorem (6, 69).

Besides size consistency, XVSCF has the following remarkable properties. The effective one-mode potential of XVSCF is quadratic,

$$V_i(Q_i) = \tilde{E}_0 + \frac{1}{2}\tilde{F}_{ii}\,Q_i^2, \quad (55)$$

where

$$\tilde{F}_{ii} = F_{ii} + \frac{1}{2}\sum_{j\neq i}^{n} F_{iijj}\left\langle\varphi_j|Q_j^2|\varphi_j\right\rangle + \frac{1}{2!2^2}\sum_{j,k\neq i}^{n} F_{iijjkk}\left\langle\varphi_j|Q_j^2|\varphi_j\right\rangle\left\langle\varphi_k|Q_k^2|\varphi_k\right\rangle + \cdots, \quad (56)$$

and $\tilde{E}_0$ is given elsewhere (69). This lends the XVSCF equation to analytical solution without any need for a basis-set expansion of modals or matrix diagonalization, while, however, still involving a self-consistent procedure. The XVSCF modal is therefore a harmonic-oscillator wave function with the XVSCF frequency,

$$\omega = \tilde{F}_{ii}^{1/2}, \quad (57)$$

which can be interpreted as the intensive fundamental transition frequency of the i-th mode. We have implemented XVSCF for molecules and demonstrated that as molecules become larger, VSCF results approach those for XVSCF, whereas XVSCF is many orders of magnitude faster than VSCF.

Size-consistent VMP and VCC based on XVSCF have also been proposed for anharmonic lattice vibrations (6).

4.2. Reciprocal-Space Downsampling Algorithms

In the proof of extensivity, we have switched between the delocalized (canonical HF spin-orbital) and localized (atomic spin-orbital) bases, depending on the effective interaction under consideration. These two bases are related to each other by Equation 18, which is more or less a Fourier transform. A method that is invariant under a unitary basis transformation in one basis is mathematically equivalent to the one in another basis; we should then select the basis that offers the greatest convenience and efficiency for a given problem. Also, a useful algorithm in one basis may translate to an equally useful algorithm in another basis.

The key idea of most fast (linear-scaling) electronic-structure methods is the distance-based truncation of molecular integrals or excitation amplitudes expressed in the basis of spatially localized functions. The corresponding algorithm in the delocalized basis is the downsampling of wave

vectors in the reciprocal-space integrations (40, 56, 70). One way to see this is to invoke Shannon's sampling theorem (71), which states that a Fourier transform of $f(x)$ that has a nonzero amplitude only at $|x| < \sigma$ can be exactly carried out by a discrete Fourier transform with a sampling rate of $1/2\sigma$. In other words, the farther an interaction reaches in real space, the greater the number of wave vector sampling points one needs to accurately reproduce the interaction in the reciprocal space.

In a nonmetal, the slowest decaying effective interaction is the Coulomb interaction (as $1/r^3$), whose lattice sum enters HF, whereas the correlation interaction, which is generally more expensive to compute, decays considerably faster (as $1/r^6$). This realization has led us to propose the mod-n downsampling scheme (40, 56, 70), in which we use sufficiently many wave vector sampling points at the HF step but a much smaller number of points in the subsequent electron-correlation calculations. In other words, we downsample wave vectors on an evenly spaced grid by a uniform rate of n only in the reciprocal-space integrations of electron-correlation calculations. It should be emphasized that this approximation has the strong physical justification given above.

The MP2 correlation correction in the mod-n approximation (40, 56, 70) is given by

$$E_{\mathrm{MP}}^{(2)} = \frac{1}{4} \sum_{p,q,r,s} \sum_{\boldsymbol{k}_p}^{V/n} \sum_{\boldsymbol{k}_q}^{V/n} \sum_{\boldsymbol{k}_r}^{V/n} \sum_{\boldsymbol{k}_s}^{V/n} w_{\boldsymbol{k}_p,\boldsymbol{k}_q,\boldsymbol{k}_r,\boldsymbol{k}_s} n_{p\boldsymbol{k}_p} n_{q\boldsymbol{k}_q} \bar{n}_{r\boldsymbol{k}_r} \bar{n}_{s\boldsymbol{k}_s} \frac{v_{p\boldsymbol{k}_p q\boldsymbol{k}_q}^{r\boldsymbol{k}_r s\boldsymbol{k}_s} v_{r\boldsymbol{k}_r s\boldsymbol{k}_s}^{p\boldsymbol{k}_p q\boldsymbol{k}_q}}{f_{p\boldsymbol{k}_p}^{p\boldsymbol{k}_p} + f_{q\boldsymbol{k}_q}^{q\boldsymbol{k}_q} - f_{r\boldsymbol{k}_r}^{r\boldsymbol{k}_r} - f_{s\boldsymbol{k}_s}^{s\boldsymbol{k}_s}}, \tag{58}$$

where V/n on a summation symbol indicates that the summation runs only over every n-th wave vector and the quadrature weight, w, takes the value

$$w_{\boldsymbol{k}_p,\boldsymbol{k}_q,\boldsymbol{k}_r,\boldsymbol{k}_s} = n^3 \tag{59}$$

if the momentum conservation condition, Equation 34, is satisfied by the downsampled set of wave vectors; otherwise it is zero. The significance of the presence of the weight, w, is twofold. First, this is necessary for the above expression to remain size consistent. Second, it compensates for the neglected correlation contributions from the unsampled wave vectors in an average way. This is in contrast with the schemes that compress the spaces of orbitals, molecular integrals, or excitation amplitudes and then simply throw away correlation contributions from "unimportant" members of these quantities without restoring them approximately (72–74). With the weight, the mod-n scheme has been shown to recover 94–103% of correlation energies of 1D solids, even when it discards 99.98% of contributions considered in the conventional algorithm and brings an 80-fold speedup of the MP2 step (40, 70).

The mod-n scheme has been applied to MP3 and CCSD (56). It accelerates by two orders of magnitude CCSD for 1D solids, making it routine for the first time. The mod-n MP2, MP3, and CCSD methods have been applied to the PES of polyethylene in anharmonic frequency calculations of its infrared- and Raman-active (namely, $\boldsymbol{k} = \boldsymbol{0}$) lattice vibrations (56). The mean absolute deviations from the observed frequencies are 47 (MP2), 46 (MP3), and 34 (CCSD) cm^{-1} without any empirical scaling of the calculated force constants or frequencies. The mod-n MP2 method has also been applied to quasi-particle energy bands and energy density of states of polyethylene and polyacetylene (40). The calculated results are in quantitative agreement with the observed (angle-resolved) photoelectron spectra.

In the mod-n scheme, wave vectors in each band are downsampled at the same rate of n. This is not mandatory and we can in fact downsample higher-lying unoccupied bands and lower-lying occupied bands at an increasingly greater rate. When the downsampling rate is set to increase exponentially, the total number of states that need to be included in the lattice sums of electron-correlation calculations increases only logarithmically with respect to the number of bands or basis functions in a unit cell. We have combined this idea with MP2 for 1D solids, introducing

the log-*n* MP2 method (75). Unlike mod-*n* MP2, which achieves an impressive, size-independent speedup, the speedup of log-*n* MP2 increases with the increasing size of the unit cell because added higher-lying unoccupied bands and lower-lying occupied bands are downsampled at a progressively greater rate. In other words, log-*n* MP2 has superior scaling of computational cost. Its energy is given by

$$E_{\mathrm{MP}}^{(2)} = \frac{1}{4} \sum_{p,q,r,s} \sum_{\boldsymbol{k}_p}^{\log V} \sum_{\boldsymbol{k}_q}^{\log V} \sum_{\boldsymbol{k}_r}^{\log V} \sum_{\boldsymbol{k}_s}^{\log V} w_{\boldsymbol{k}_p,\boldsymbol{k}_q,\boldsymbol{k}_r,\boldsymbol{k}_s}^{p,q,r,s} n_{p\boldsymbol{k}_p} n_{q\boldsymbol{k}_q} \bar{n}_{r\boldsymbol{k}_r} \bar{n}_{s\boldsymbol{k}_s} \frac{v_{p\boldsymbol{k}_p q\boldsymbol{k}_q}^{r\boldsymbol{k}_r s\boldsymbol{k}_s} v_{r\boldsymbol{k}_r s\boldsymbol{k}_s}^{p\boldsymbol{k}_p q\boldsymbol{k}_q}}{f_{p\boldsymbol{k}_p}^{p\boldsymbol{k}_p} + f_{q\boldsymbol{k}_q}^{q\boldsymbol{k}_q} - f_{r\boldsymbol{k}_r}^{r\boldsymbol{k}_r} - f_{s\boldsymbol{k}_s}^{s\boldsymbol{k}_s}}, \quad (60)$$

where log V on a summation symbol (figuratively) indicates that the summation runs over an exponentially downsampled grid of wave vectors. Again, weight, w, is necessary to maintain size consistency and to compensate for unsampled contributions. We have found an appropriate expression for it (75) to be

$$w_{\boldsymbol{k}_p,\boldsymbol{k}_q,\boldsymbol{k}_r,\boldsymbol{k}_s}^{p,q,r,s} = \max(n_p n_q n_r, n_p n_q n_s, n_p n_r n_s, n_q n_r n_s), \quad (61)$$

if Equation 34 is satisfied; otherwise the weight is zero, where n_p denotes the downsampling rate of the p-th band. It is essential that we connect discrete band energies correctly by resolving all real and avoided crossings for this scheme to work.

4.3. Hybrid CC/MP Method

The core idea of the log-*n* MP2 method is that we should treat the bands near the Fermi surface and the others differently, namely, put more computational efforts on the frontier bands and much less on the others. We can go a step further and apply higher-accuracy methods such as CCSD only to the frontier bands and lower-accuracy methods such as MP2 to the rest. The corresponding hybrid in the real space, applying CCSD and MP2 for short- and long-range interactions, respectively, was proposed and implemented for molecules by Schütz & Werner (76). The hybrid in the energy space for molecules was introduced by Nooijen (77) and studied by Bochevarov et al. (78, 79).

We have extended the hybrid CC/MP method of Nooijen to 1D solids (80). We apply CCSD only to the frontier bands, which are responsible for the possible divergence of MP2 in metals, while treating other bands by less expensive MP2. An efficient implementation of this method requires a complete revision of the working equations of CCSD such that matrix multiplications of the molecular integrals and first-order amplitudes, which do not vary during an iterative solution of the CCSD equations, are isolated and executed before the iteration. We have proposed such a revised set of equations. The bands need to be connected correctly. The hybrid CCSD/MP2 method has been shown to recover 98% of CCSD correlation energy or approximately half of the difference between CCSD and MP2 at less than a tenth of the usual CCSD cost for polyacetylene (80).

4.4. Binary-Interaction Method

For systems that have essentially localized chemistry, we may switch to a local basis. Classes of systems whose interactions are most localized are molecular clusters, crystals, and liquids. They include such important systems as water and ice. They are distinguished from other clusters, solids, and liquids in that they maintain molecular identities of the constituents. We can use molecular orbitals and energies of the constituents as a convenient computational basis for the description of the whole system.

We have proposed a high-accuracy electron-correlation method for routine first-principles determination of energies, structures, and phonon dispersion of molecular crystals. This

binary-interaction method (81–85) approximates the total energy per unit cell of a crystal, $U = E/V$, by

$$U = \sum_i E_{i(\mathbf{0})} + \sum_{i<j} \left(E_{i(\mathbf{0})j(\mathbf{0})} - E_{i(\mathbf{0})} - E_{j(\mathbf{0})} \right) + \frac{1}{2} \sum_{\mathbf{m}}^{V} (1 - \delta_{\mathbf{m}0}) \sum_{i,j} \left(E_{i(\mathbf{0})j(\mathbf{m})} - E_{i(\mathbf{0})} - E_{j(\mathbf{m})} \right), \quad (62)$$

where $E_{j(\mathbf{m})}$ denotes the energy of the j-th constituent molecule in unit cell $\mathbf{m}$ and $E_{i(\mathbf{0})j(\mathbf{m})}$ the energy of the dimer consisting of the i-th molecule in unit cell $\mathbf{0}$ and the j-th molecule in unit cell $\mathbf{m}$. These molecules are embedded in the electrostatic field of the rest of the molecules in the crystal determined to be self-consistent with one another. This is the second-lowest member in the series of many-body expansion of energy; three-body, four-body, etc., energies can be included, if necessary, to increase the fidelity of the simulations at an increased computational cost. There are many similar methods and we do not attempt to cite all relevant studies here except to note that ours is a direct simplification of Kitaura et al.'s (86) pair-interaction method, which is the predecessor of their highly successful fragment molecular orbital method (87).

The total energy is manifestly extensive in this local-basis method regardless of which electron-correlation method is used to evaluate $E_{j(\mathbf{m})}$ and $E_{i(\mathbf{0})j(\mathbf{m})}$. Even a non-size-extensive, truncated CI can be used! A combination of MP or CC with the binary-interaction method can describe all chemical interactions in molecular crystals, with their strengths spanning at least three orders of magnitude. The basis-set superposition errors (BSSE) in weak interactions such as hydrogen-bond and dispersion interactions can be removed effectively by a counterpoise method (82). Excited states in a condensed phase can also be studied (81).

The first and second derivatives of U with respect to the atomic coordinates can be readily obtained as the corresponding sum of the derivatives of molecules and dimers (81, 88), which today can be computed analytically in electronic structure programs for molecules. Furthermore, the derivatives with respect to coordinates unique to crystals—lattice parameters (a, b, and c)—can also be computed (83) efficiently as

$$\frac{\partial U}{\partial a} = \sum_{\mathbf{m}}^{V} m_x \sum_{i,j} \sum_{\gamma} \left\{ \frac{\partial E_{i(\mathbf{0})j(\mathbf{m})}}{\partial x^{\gamma}_{j(\mathbf{m})}} - \frac{\partial E_{j(\mathbf{m})}}{\partial x^{\gamma}_{j(\mathbf{m})}} \right\}, \quad (63)$$

where $x^{\gamma}_{j(\mathbf{m})}$ denotes the x coordinate of the γ-th atom in the j-th molecule in unit cell $\mathbf{m}$. The derivatives with respect to b or c are obtained by evaluating the same expression with x being replaced by y or z, respectively. These are helpful in determining the structures and Young's modulus of molecular crystals. In a step toward integrating electronic structure theory and thermodynamics, we also consider the enthalpy per unit cell, $H = U + P(abc)$, where P is pressure, if the lattice is orthorhombic. Its derivatives with respect to atomic coordinates and lattice parameters can be easily computed, e.g.,

$$\frac{\partial H}{\partial a} = \frac{\partial U}{\partial a} + P(bc). \quad (64)$$

This has proved useful when studying pressure dependence of the structure and phonons (O. Sode & S. Hirata, manuscript in preparation).

The binary-interaction method at the MP2 and CCSD levels has been applied to solid formic acid (83), which is of interest in relation to the structure of hydrogen-bonded solid, liquid, and aerosols, phase transitions, polymorphism, concerted proton transfer, etc. Accurate energies with BSSE corrections, structural parameters, and frequencies and reliable assignments of infrared, Raman, and inelastic neutron scattering spectral bands have been obtained for three conformers (α, β_1, and β_2) of the 1D chains. The results suggest that the observed diffraction and spectroscopic data are consistent with the pristine β_1 form and that the mysterious infrared band splitting can be

assigned to the in-phase and out-of-phase vibrations of adjacent formic acid molecules rather than to the speculated polymorphism (89). Spectral features expected from the α and β_2 forms have also been shown to be incompatible with the observed Raman and inelastic neutron scattering in the low-energy region.

VCI: vibrational configuration interaction

The 3D structure of solid hydrogen fluoride has been a subject of debate. Four prior experimental studies (90–93) were split among three possible structures, polar, nonpolar, and disordered, whereas three previous computational studies (94–96) were also inconclusive and divided between polar and nonpolar structures. Our binary-interaction calculations (85) at the MP2 level with the BSSE correction have been decisive in favoring the nonpolar structure, ending the controversy. We have also studied the pressure dependence of the volume, infrared- and Raman-active vibrational frequencies, and phonon dispersion and density of states using the technique discussed above. In the 1D model of solid hydrogen fluoride, we can easily raise the level of electronic structure theory to CCSD and CCSD with a noniterative connected triples correction and that of a vibrational treatment to vibrational configuration interaction (VCI) (84). This calculation has reproduced the observed frequencies of the Raman bands of solid hydrogen fluoride with the mean absolute deviation of 55 cm^{-1} without empirical scaling.

SUMMARY POINTS

1. The systematic, diagrammatic many-body methods such as MP and CC are beginning to be applied to solids, demonstrating their unprecedented potential in achieving predictive accuracy in such applications.
2. The electronic and vibrational methods whose accuracy can be controlled and maintained across the whole range of system size can only be designed with the essential aid of (diagrammatic) size-consistency criteria and an understanding of the size dependence of thermodynamic observables that these methods are meant to predict.
3. The computational cost of these methods and the feasibility of their applications to solids and liquids are ultimately determined by the asymptotes of the effective chemical interactions.
4. The proof of extensivity of energy, the asymptotes of effective chemical interactions, and the diagrammatic criteria of size consistency and a guideline for size-consistent designs have been given. Several novel theories and algorithms have been proposed on this basis.

DISCLOSURE STATEMENT

The authors are not aware of any affiliations, memberships, funding, or financial holdings that might be perceived as affecting the objectivity of this review.

ACKNOWLEDGMENTS

This work has been supported by the U.S. National Science Foundation (CHE-1118616 and OCI-1102418) and the U.S. Department of Energy (DE-FG02-11ER16211). S.H. is a Camille Dreyfus Teacher-Scholar of the Camille and Henry Dreyfus Foundation, Inc., a Scialog Fellow of the Research Corporation for Science Advancement, and an Alumni Research Scholar of the University of Illinois. M.K. is a University Block Grant Fellow of the University of Illinois. O.S. is

a Roger Adams Fellow of the University of Illinois and a GAANN Fellow of the U.S. Department of Education.

LITERATURE CITED

1. Helgaker T, Klopper W, Tew DP. 2008. Quantitative quantum chemistry. *Mol. Phys.* 106:2107–43
2. Hirata S. 2009. Quantum chemistry of macromolecules and solids. *Phys. Chem. Chem. Phys.* 11:8397–412
3. Sinnokrot MO, Sherrill CD. 2006. High-accuracy quantum mechanical studies of π-π interactions in benzene dimers. *J. Phys. Chem. A* 110:10656–68
4. Ringer AL, Sherrill CD. 2008. First principles computation of lattice energies of organic solids: the benzene crystal. *Chem. Eur. J.* 14:2542–47
5. Christiansen O. 2007. Vibrational structure theory: new vibrational wave function methods for calculation of anharmonic vibrational energies and vibrational contributions to molecular properties. *Phys. Chem. Chem. Phys.* 9:2942–53
6. **Hirata S, Keçeli M, Yagi K. 2010. First-principles theories for anharmonic lattice vibrations. *J. Chem. Phys.* 133:034109**
7. Szabo A, Ostlund NS. 1989. *Modern Quantum Chemistry*. New York: McGraw-Hill
8. **Bartlett RJ. 1981. Many-body perturbation theory and coupled-cluster theory for electron correlation in molecules. *Annu. Rev. Phys. Chem.* 32:359–401**
9. Nooijen M, Shamasundar KR, Mukherjee D. 2005. Reflections on size-extensivity, size-consistency and generalized extensivity in many-body theory. *Mol. Phys.* 103:2277–98
10. **Hirata S. 2011. Thermodynamic limit and size-consistent design. *Theor. Chem. Acc.* 129:727–46**
11. Chandler D. 1987. *Introduction to Modern Statistical Mechanics*. New York: Oxford Univ. Press
12. Lieb EH, Seiringer R. 2010. *The Stability of Matter in Quantum Mechanics*. Cambridge, UK: Cambridge Univ. Press
13. Lebowitz JL, Lieb EH. 1969. Existence of thermodynamics for real matter with Coulomb forces. *Phys. Rev. Lett.* 22:631–34
14. Fefferman C. 1985. The thermodynamic limit for a crystal. *Commun. Math. Phys.* 98:289–311
15. Hainzl C, Lewin M, Solovej JP. 2009. The thermodynamic limit of quantum Coulomb systems. Part I. General theory. *Adv. Math.* 221:454–87
16. Hainzl C, Lewin M, Solovej JP. 2009. The thermodynamic limit of quantum Coulomb systems. Part II. Applications. *Adv. Math.* 221:488–546
17. Fisher ME, Ruelle D. 1966. Stability of many-particle systems. *J. Math. Phys.* 7:260–70
18. Dyson FJ, Lenard A. 1967. Stability of matter. I. *J. Math. Phys.* 8:423–34
19. Dyson FJ, Lenard A. 1968. Stability of matter. II. *J. Math. Phys.* 9:698–711
20. Lieb EH, Lebowitz JL. 1972. Constitution of matter: existence of thermodynamics for systems composed of electrons and nuclei. *Adv. Math.* 9:316–98
21. Lieb EH. 1976. Stability of matter. *Rev. Mod. Phys.* 48:553–69
22. Lieb EH, Simon B. 1977. The Hartree-Fock theory for Coulomb systems. *Commun. Math. Phys.* 53:185–94
23. Thirring W. 1990. Stability of matter. *Found. Phys.* 20:1103–10
24. Tsallis C. 2001. Nonextensive statistical mechanics and thermodynamics: historical background and present status. In *Nonextensive Statistical Mechanics and Its Applications*, ed. S Abe, Y Okamoto, pp. 3–98. Berlin: Springer
25. **Delhalle J, Piela L, Brédas JL, André JM. 1980. Multipole expansion in tight-binding Hartree–Fock calculations for infinite-model polymers. *Phys. Rev. B* 22:6254–67**
26. des Cloizeaux J. 1964. Energy bands and projection operators in a crystal: analytic and asymptotic properties. *Phys. Rev. A* 135:685–97
27. **Monkhorst HJ, Kertesz M. 1981. Exact-exchange asymptotics in polymer Hartree–Fock calculations. *Phys. Rev. B* 24:3015–24**
28. **Piela L, André JM, Fripiat JG, Delhalle J. 1981. On the behavior of exchange in restricted Hartree–Fock–Roothaan calculations for periodic polymers. *Chem. Phys. Lett.* 77:143–50**

6. Size-consistent formulations of vibrational methods based on many-body techniques established in electronic structure theory.

8. An authoritative review of diagrammatic many-body methods by the steadfast advocate of the significance of size consistency.

10. An in-depth discussion of size consistency and diagrammatic theorems.

25. The first physically sound scheme for lattice sum truncation, which can be combined with multipole expansions of long-range interactions.

27, 28. These studies showed that the exchange interaction decays exponentially in an insulator.

29. **Pisani C, Aprà E, Causà M. 1990. Density matrix of crystalline systems. I. Long-range behavior and related computational problems. *Int. J. Quantum Chem.* 38:395–417**
30. March NH, Young WH, Sampanthar S. 1967. *The Many-Body Problem in Quantum Mechanics*. New York: Cambridge Univ. Press
31. André JM, Delhalle J, Brédas JL. 1991. *Quantum Chemistry Aided Design of Organic Polymers: An Introduction to the Quantum Chemistry of Polymers and Its Applications*. Singapore: World Sci.
32. Ohnishi YY, Hirata S. 2011. Charge-consistent redefinition of Fock integrals. *Chem. Phys.* In press
33. Shavitt I, Bartlett RJ. 2009. *Many-Body Methods in Chemistry and Physics*. New York: Cambridge Univ. Press
34. **Kunz AB. 1972. Electronic polarons in nonmetals. *Phys. Rev. B* 6:606–15**
35. Suhai S. 1983. Bond alternation in infinite polyene: Peierls distortion reduced by electron correlation. *Chem. Phys. Lett.* 96:619–25
36. Suhai S. 1983. Quasiparticle energy-band structures in semiconducting polymers: correlation effects on the band gap in polyacetylene. *Phys. Rev. B* 27:3506–18
37. Sun JQ, Bartlett RJ. 1996. Second-order many-body perturbation-theory calculations in extended systems. *J. Chem. Phys.* 104:8553–65
38. Ayala P, Scuseria GE. 1999. Linear scaling second-order Møller–Plesset theory in the atomic orbital basis for large molecular systems. *J. Chem. Phys.* 110:3660–71
39. Hirata S, Podeszwa R, Tobita M, Bartlett RJ. 2004. Coupled-cluster singles and doubles for extended systems. *J. Chem. Phys.* 120:2581–92
40. Hirata S, Shimazaki T. 2009. Fast second-order many-body perturbation method for extended systems. *Phys. Rev. B* 80:085118
41. Marsman M, Grüneis A, Paier J, Kresse G. 2009. Second-order Møller–Plesset perturbation theory applied to extended systems. I. Within the projector-augmented-wave formalism using a plane wave basis set. *J. Chem. Phys.* 130:184103
42. Grüneis A, Marsman M, Kresse G. 2010. Making the random phase approximation to electronic correlation accurate. *J. Chem. Phys.* 133:074107
43. Brueckner KA. 1955. Many-body problem for strongly interacting particles. II. Linked cluster expansion. *Phys. Rev.* 100:36–45
44. Goldstone J. 1957. Derivation of the Brueckner many-body theory. *Proc. R. Soc. Lond. A* 239:267–79
45. Gell-Mann M, Brueckner KA. 1957. Correlation energy of an electron gas at high density. *Phys. Rev.* 106:364–68
46. Bishop RF, Lührmann KH. 1978. Electron correlations. I. Ground-state results in high-density regime. *Phys. Rev. B* 17:3757–80
47. Bishop RF. 1991. An overview of coupled cluster theory and its applications in physics. *Theor. Chim. Acta* 80:95–148
48. Bohm D, Pines D. 1951. A collective description of electron interactions. I. Magnetic interactions. *Phys. Rev.* 82:625–34
49. Langreth DC, Perdew JP. 1977. Exchange-correlation energy of a metallic surface: wave-vector analysis. *Phys. Rev. B* 15:2884–901
50. Furche F. 2008. Developing the random phase approximation into a practical post-Kohn–Sham correlation model. *J. Chem. Phys.* 129:114105
51. Harl J, Kresse G. 2008. Cohesive energy curves for noble gas solids calculated by adiabatic connection fluctuation-dissipation theory. *Phys. Rev. B* 77:045136
52. Harl J, Kresse G. 2009. Accurate bulk properties from approximate many-body techniques. *Phys. Rev. Lett.* 103:056401
53. Freemen DL, Karplus M. 1976. Many-body perturbation theory applied to molecules: analysis and correlation energy calculation for Li_2, N_2, and H_3. *J. Chem. Phys.* 64:2641–59
54. Scuseria GE, Henderson TM, Sorensen DC. 2008. The ground state correlation energy of the random phase approximation from a ring coupled cluster doubles approach. *J. Chem. Phys.* 129:231101
55. Suhai S. 1994. Electron correlation in extended systems: fourth-order many-body perturbation theory and density-functional methods applied to an infinite chain of hydrogen atoms. *Phys. Rev. B* 50:14791–801

29. This study showed that the density matrix elements decay as an inverse square of distance in a 3D metal.

34. A pioneering application of MP2 to crystals.

56. Keçeli M, Hirata S. 2010. Fast coupled-cluster singles and doubles for extended systems: application to the anharmonic vibrational frequencies of polyethylene in the Γ approximation. *Phys. Rev. B* 82:115107
57. Shiozaki T, Hirata S. 2010. Explicitly correlated second-order Møller–Plesset perturbation method for extended systems. *J. Chem. Phys.* 132:151101
58. Vračko MG, Zaider M. 1992. A calculation of exciton energies in periodic systems with helical symmetry: application to a hydrogen-fluoride chain. *Int. J. Quantum Chem.* 43:321–26
59. Vračko MG, Zaider M. 1993. A study of excited states in trans-polyacetylene in the Hartree–Fock, Tamm–Dancoff, and random-phase-approximation. *Int. J. Quantum Chem.* 47:119–27
60. Vračko M, Champagne B, Mosley DH, André JM. 1995. Study of excited states of polyethylene in the Hartree–Fock, Tamm–Dancoff, and random-phase approximations. *J. Chem. Phys.* 102:6831–36
61. Hirata S, Head-Gordon M, Bartlett RJ. 1999. Configuration interaction singles, time-dependent Hartree–Fock, and time-dependent density functional theory for the electronic excited states of extended systems. *J. Chem. Phys.* 111:10774–86
62. Katagiri H. 2005. Equation-of-motion coupled-cluster study on exciton states of polyethylene with periodic boundary condition. *J. Chem. Phys.* 122:224901
63. Bowman JM. 1978. Self-consistent field energies and wavefunctions for coupled oscillators. *J. Chem. Phys.* 68:608–10
64. Bowman JM. 1986. The self-consistent-field approach to polyatomic vibrations. *Acc. Chem. Res.* 19:202–8
65. Gerber RB, Ratner MA. 1988. Self-consistent-field methods for vibrational excitations in polyatomic systems. *Adv. Chem. Phys.* 70:97–132
66. Norris LS, Ratner MA, Roitberg AE, Gerber RB. 1996. Møller–Plesset perturbation theory applied to vibrational problems. *J. Chem. Phys.* 105:11261–67
67. Christiansen O. 2003. Møller–Plesset perturbation theory for vibrational wave functions. *J. Chem. Phys.* 119:5773–81
68. Christiansen O. 2004. Vibrational coupled cluster theory. *J. Chem. Phys.* 120:2149–59
69. Keçeli M, Hirata S. 2011. Size-extensive vibrational self-consistent field method. *J. Chem. Phys.* 135:134108
70. Shimazaki T, Hirata S. 2009. On the Brillouin-zone integrations in second-order many-body perturbation calculations for extended systems of one-dimensional periodicity. *Int. J. Quantum Chem.* 109:2953–59
71. Shannon CE. 1949. Communication in the presence of noise. *Proc. IRE* 37:10–21
72. Koch H, de Merás AS, Pedersen TB. 2003. Reduced scaling in electronic structure calculations using Cholesky decompositions. *J. Chem. Phys.* 118:9481–84
73. Kinoshita T, Hino O, Bartlett RJ. 2003. Singular value decomposition approach for the approximate coupled-cluster method. *J. Chem. Phys.* 119:7756–62
74. Taube AG, Bartlett RJ. 2005. Frozen natural orbitals: systematic basis set truncation for coupled-cluster theory. *Coll. Czech. Chem. Commun.* 70:837–50
75. Ohnishi YY, Hirata S. 2010. Logarithm second-order many-body perturbation method for extended systems. *J. Chem. Phys.* 133:034106
76. Schütz M, Werner HJ. 2001. Low-order scaling local electron correlation methods. IV. Linear scaling local coupled-cluster (LCCSD). *J. Chem. Phys.* 114:661–81
77. Nooijen M. 1999. Combining coupled cluster and perturbation theory. *J. Chem. Phys.* 111:10815–26
78. Bochevarov AD, Sherrill CD. 2005. Hybrid correlation models based on active-space partitioning: correcting second-order Møller–Plesset perturbation theory for bond-breaking reactions. *J. Chem. Phys.* 122:234110
79. Bochevarov AD, Temelso B, Sherrill CD. 2006. Hybrid correlation models based on active-space partitioning: seeking accurate $O(N^5)$ ab initio methods for bond breaking. *J. Chem. Phys.* 125:054109
80. Ohnishi YY, Hirata S. 2011. Hybrid coupled-cluster and perturbation method for extended systems. *J. Chem. Phys.* 135:094108
81. Hirata S, Valiev M, Dupuis M, Xantheas SS, Sugiki S, Sekino H. 2005. Fast electron correlation methods for molecular clusters in the ground and excited states. *Mol. Phys.* 103:2255–65
82. Kamiya M, Hirata S, Valiev M. 2008. Fast electron correlation methods for molecular clusters without basis set superposition errors. *J. Chem. Phys.* 128:074103

83. Hirata S. 2008. Fast electron-correlation methods for molecular crystals: an application to the α, β_1, and β_2 polymorphs of solid formic acid. *J. Chem. Phys.* 129:204104
84. Sode O, Keçeli M, Hirata S, Yagi K. 2009. Coupled-cluster and many-body perturbation study of energies, structures, and phonon dispersions of solid hydrogen fluoride. *Int. J. Quantum Chem.* 109:1928–39
85. Sode O, Hirata S. 2010. Second-order many-body perturbation study of solid hydrogen fluoride. *J. Phys. Chem. A* 114:8873–77
86. Kitaura K, Sawai T, Asada T, Nakano T, Uebayasi M. 1999. Pair interaction molecular orbital method: an approximate computational method for molecular interactions. *Chem. Phys. Lett.* 312:319–24
87. Kitaura K, Ikeo E, Asada T, Nakano T, Uebayasi M. 1999. Fragment molecular orbital method: an approximate computational method for large molecules. *Chem. Phys. Lett.* 313:701–6
88. Kitaura K, Sugiki SI, Nakano T, Komeiji Y, Uebayasi M. 2001. Fragment molecular orbital method: analytical energy gradients. *Chem. Phys. Lett.* 336:163–70
89. Tubino R, Zerbi G. 1970. Phonon curves and frequency distribution for hydrogen-bonded systems: β modification of solid HCOOH, HCOOD, and DCOOH. *J. Chem. Phys.* 53:1428–32
90. Giguère PA, Zengin N. 1958. Spectre infrarouge de HF à l'état cristallin. *Can. J. Chem.* 36:1013–19
91. Kittelberger JS, Hornig DF. 1967. Vibrational spectrum of crystalline HF and DF. *J. Chem. Phys.* 46:3099–108
92. Habuda SP, Gagarinsky YV. 1971. Nuclear magnetic resonance data on proton positions in solid HF. *Acta Crystallogr. B* 27:1677–78
93. Johnson MW, Sándor E, Arzi E. 1975. Crystal structure of deuterium fluoride. *Acta Crystallogr. B* 31:1998–2003
94. Bacon J, Santry DP. 1972. Molecular-orbital theory for infinite systems: hydrogen-bonded molecular crystals. *J. Chem. Phys.* 56:2011–16
95. Ángyán JG, Silvi B. 1987. Electrostatic interactions in three-dimensional solids: self-consistent Madelung potential (SCMP) approach. *J. Chem. Phys.* 86:6957–66
96. Panas I. 1993. On the solid state of hydrogen fluoride: a self-consistent crystal-field study. *Int. J. Quantum Chem.* 46:109–18

83. An early application of fragment electron-correlation methods to crystals.

87. This successful fragment method prompted a surge of development of many similar methods.

Annual Review of
Physical Chemistry
Volume 63, 2012

Contents

Indexes

Errata

An online log of corrections to Annual Review of Physical Chemistry chapters (if any, 1997 to the present) may be found at http://physchem.AnnualReviews.org/errata.shtml